Simple Viscous-Inviscid Aerodynamic Analysis of Two-Dimensional Augmentors

D. A. Tavella* and L. Roberts†
Stanford University, Stanford, California

A theory for the computation of two-dimensional thrust augmentor performance has been developed. The flowfield is assumed to be incompressible, of uniform density, and statistically steady. The flowfield in and around the augmentor is assumed to consist of an outer inviscid part and an inner viscous part. The outer field is computed analytically and then matched with the inner field, which is computed by integral methods. Some of the theoretical results are compared with recently acquired experimental data.

Nomenclature

$\{A\},\{B\}$	= matrix and right-hand side of reduced equations
b	= characteristic width of turbulent region
h	= shroud inner half-width
l	= shroud length
k	= eddy viscosity scaling constant
m_j	= primary jet momentum
p	= pressure
q	= shroud perturbation source intensity
q_p	= primary jet sink intensity
T	= shroud-associated thrust
u,v	= x,y velocity components
U_b	= Borda velocity
u_0	= outer limit of viscous solution
u_1	= excess velocity in viscous region
$\hat{u}$	= approximation to viscous solution
V	= complex velocity
z,w	= complex coordinates in physical ($z=\bar{x}+i\bar{y}$), transformed plane ($w=\zeta+i\eta$)
x,y	= coordinates in viscous solution
$\bar{x}_j,\zeta_j$	= primary jet origin in physical, transformed plane
$\bar{x}^*,\zeta^*$	= wedge length in physical, transformed plane
α	= $-\log(2)$
γ	= constant in perturbation expansion for $\bar{x}\to 0$
Γ	= x-momentum equation operator
δ	= wedge angle in augmentor shroud
ν_t	= kinematic eddy viscosity
ρ	= density
τ	= Reynold's stress in two-dimensional boundary-layer approximation
φ	= thrust augmentation
$\phi,\phi_b,\phi_p,\phi_e$	= velocity potential of outer flow, channel flow, primary jet entrainment, exhaust entrainment
ψ	= stream function
Ω	= y projection of diffuser inner surface
ϵf	= shroud perturbation in physical plane

Superscripts

[$\bar{}$]	= variable is evaluated in the w plane
[$\dot{}$]	= derivative with respect to argument

Presented as Paper 84-0281 at the AIAA 22nd Aerospace Sciences, Reno, NV, Jan. 9-12, 1984; received Dec. 15, 1984; revision received Nov. 25, 1986.

*Research Associate, Joint Institute for Aeronautics and Astronautics, Department of Aeronautics and Astronautics. Member AIAA.

†Director, Joint Institute for Aeronautics and Astronautics, Department of Aeronautics and Astronautics. Fellow AIAA.

Introduction

A THRUST augmentor is a device where a high-momentum primary jet undergoes turbulent mixing with a secondary stream surrounded by a shroud. The resulting thrust produced by the jet/shroud combination is higher than the thrust that would result from the jet discharging in isolation. This augmentation of thrust arises from the induced pressure distribution on the surface of the shroud and from the fact that the primary jet discharges in an environment at lower pressure.

In this work, effort is focused on two-dimensional augmentors with incompressible, statistically steady flow. Considerable work has been devoted in recent years to the prediction of augmentor performance, as reported in a comprehensive overview by Porter and Squyers.[1] Most of the theories fall in either one of the following two categories: those that make use of conservation laws in global form, the so-called control volume approaches, and those that attempt to solve the two-dimensionality of the problem. This second category includes approaches based on the direct numerical solution of the conservation equations by finite differences and those based on integral methods, such as the study presented here.

An essential element in augmentor flow analysis is the viscous-inviscid interaction between the turbulent primary flow and the turbulence-free secondary flow in regions where the mixing does not extend all across the shroud cross section. In earlier theories this interaction was considerably simplified by assuming that the still-unmixed secondary flow was essentially uniform, the pressure being constant on any cross section of the shroud.[2,3] This assumption is acceptable in the case of elongated jet pumps in which the primary nozzle is located well inside the shroud, where the secondary flow can justifiably be considered uniform. The case of ejectors with uniform secondary flow was treated by Bevilaqua and McCullough[3] with an integral method for the viscous flow. In this approach, free-jet data were used to determine the entrainment rate into the primary jet. In the case of augmentors for aeronautical applications, the primary nozzle may be located outside the shroud or close enough to the inlet such that the inviscid flow drawn into the device can by no means be considered uniform. Bevilaqua[4] also developed a theory where the viscous-inviscid interaction is taken into account by dividing the flowfield into an external flow, which was solved with a panel method, and by characterizing the internal flow in terms of its entrainment properties. Improving on the characterization of the viscous field, Bevilaqua et al.[5,6] formulated an approach where the entrainment of the viscous flowfield is computed by solving the primary jet flow by finite differences, with the external inviscid flow also represented by panels. Although these approaches capture the essential physics of augmentors, the combination of panel methods and finite differences is computationally much costlier than the procedure presented here.

In this work the viscous-inviscid approach is formulated in the simplest possible form, by solving the external inviscid field analytically and computing the internal viscous flow by an integral method. An inner/outer matching, in the boundary-layer sense, is performed between the two flowfields. The approach is developed for stationary augmentors, where the turbulent mixing region reaches the shroud walls before exiting the device. Measurements obtained by Bernard and Sorahia[7] were used to compare with the theoretical results.

Mathematical Model

The flowfield of a typical two-dimensional augmentor will be divided in three regions, as shown in Fig. 1. In region 1 a strong viscous-inviscid interaction between the primary jet flow and the inviscid flowfield takes place. In this region a viscous-inviscid matching process is required to determine both flowfields. Region 2 is composed of a transition zone between the strongly interacting viscous-inviscid fields of region 1 and a zone where the turbulent flow extends all across the channel. The upstream boundary of this region is where the secondary flow becomes fairly uniform, which depends on the shroud form. In the cases analyzed here this boundary is about half channel widths from the inlet plane. Within reasonable margins, the results are insensitive to this boundary location. At the beginning of region 2, the inner flow model resolves the flowfield all across the augmentor channel.

The pressure attains a minimum somewhere in region 1 and then increases gradually due to momentum dissipation, reaching atmospheric value at the end of region 2. Region 3 constitutes the exhaust plume, which develops as a free turbulent jet. Entrainment into the exhaust jet is not expected to be a significant factor in performance and will not be considered. Full details of the theory are given in Ref. 8.

Viscous Solution

The inner viscous solution is obtained by applying an integral method to the time-averaged flow quantities. Making use of boundary-layer assumptions and neglecting the component of stress due to molecular viscosity, the equation of conservation of momentum in the x direction is

$$\Gamma(u) = u\frac{\partial u}{\partial x} - \frac{\partial u}{\partial y}\int_0^y \frac{\partial u}{\partial x}\mathrm{d}\eta + \frac{l\mathrm{d}p}{\rho\mathrm{d}x} - \frac{l\partial\tau}{\rho\partial y} = 0 \tag{1}$$

and the equation of conservation of mass

$$\frac{\partial u}{\partial x} + \frac{\partial v}{\partial y} = 0 \tag{2}$$

A representation for $u(x,y)$ valid from the primary nozzle exit to the exhaust nozzle exit plane is postulated, as shown in Fig. 2,

$$\hat{u}(x,y) = u_0(x) + u_1(x)e^{-\alpha(y^2/b^2)} \tag{3}$$

where $u_0(x)$, $u_1(x)$, and $b(x)$ are unknown a priori. This representation implies that the boundary layers on the inner side of the augmentor walls are ignored, which in the absence of separation is not expected to introduce significant error in performance estimates.

The Reynold's stress τ is represented by a kinematic eddy viscosity model of the form

$$\frac{\tau}{\rho} = \nu_t \frac{\partial \hat{u}}{\partial y} \tag{4}$$

where ν_t is assumed to scale as $\nu_t = ku_1b$, with k a constant determined by requiring that the integral method should give $\dot{b} = 0.1$ when applied to a two-dimensional turbulent jet. This gives $k = 0.0283$. In the case of the turbulent jet developing within the augmentor, comparison between computed and measured inner flowfields suggests that the value of k should be slightly larger. Values of k of up to 0.035 can be used without visible effects on the global aspects of performance, such as total mass flux and thrust augmentation. Substituting Eqs. (3) and (4) into Eq. (1), and taking n moments of the operator $\Gamma(u)$, a system of n independent equations is obtained,

$$\int_0^{h(x)} y^n \Gamma(\hat{u})\mathrm{d}y = 0$$
$$n = 0,1,2\ldots \tag{5}$$

Equations (5) together with the equation of conservation of mass constitute a set of four nonlinear ordinary differential equations in u_0, u_1, b, p, and their derivatives. In matrix form,

$$\{A\}\begin{bmatrix}\dot{u}_0\\ \dot{u}_1\\ \dot{b}\\ \dot{p}\end{bmatrix} = \{B\} \tag{6}$$

In region 1, where the viscous-inviscid matching takes place, the system reduces to two equations for u_1 and b, since the matching conditions provide u_0 and thus p through Bernoulli's equation. In region 2, the system is solved for all four variables.

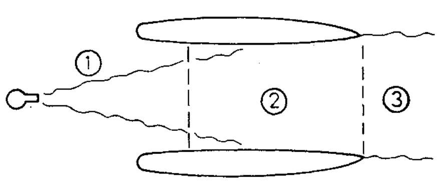

Fig. 1 Augmentor flow regions.

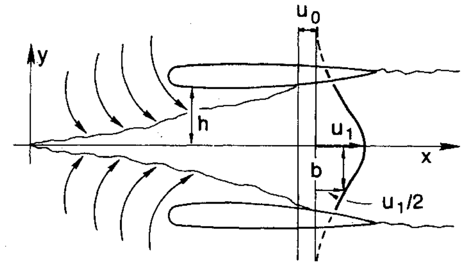

Fig. 2 Viscous solution.

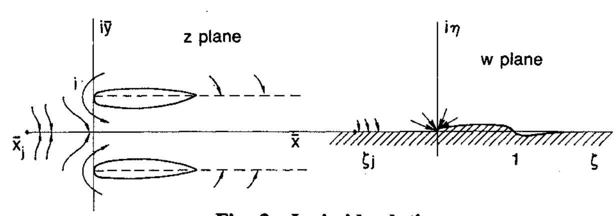

Fig. 3 Inviscid solution.

The representation given by Eq. (3) implies that the primary jet is being modeled as a source of momentum in the x direction, located at the position where $b(x)=0$. This position is a singular point that may be thought of as the virtual origin of the primary jet. The calculation of the viscous flow is started slightly downstream of the momentum source location to avoid the singular behavior.

Inviscid Solution

The inviscid solution will be found as the superposition of a basic solution, consisting of the so-called Borda mouthpiece flow, plus a perturbation on such a flow. The Borda mouthpiece flow arises when ideal fluid enters a semi-infinite channel of parallel walls under the condition that the flow inside the channel should become uniform infinitely far downstream. The complex potential of such a flow will be called ϕ_b. The perturbation on the basic flow serves a correction to deal with shrouds with shapes that deviate slightly from a straight channel. The resultant complex potential is $\phi=\phi_b+\Delta\phi_b+\phi_p+\phi_e$, where ϕ_p and ϕ_e are the potentials induced by the primary and exhaust jets and $\Delta\phi_b$ the perturbation potential. The basic solution, without separation, can be found easily by conformal mapping. The perturbation scheme is then carried out in the transformed plane. Consider a semi-infinite channel as indicated by the dotted line in Fig. 3. Due to symmetry, it is only necessary to consider the upper half of the physical plane. If the upper wall of the channel is now defined as a slit in the physical plane, the application of the Schwarz-Christofel theorem to the degenerate polygon defined by the slit and the x axis leads to the following expression, transforming the exterior of that polygon onto the upper part of the w plane:

$$z=(1/\pi)(w+\ln w+i\pi-1) \tag{7}$$

Defining U_b as the cross-sectional average of the inviscid flow velocity entering the channel, to be called the "Borda velocity," the requirement that the flow inside the channel should be uniform infinitely far downstream gives $\phi_b \to U_b z$ as $x\to\infty$ for $0<y<1$. From Eq. (7), it results

$$\tilde{\phi}_b=-(U_b/\pi)\ln w \tag{8}$$

Consider now a cowling of general shape such that its internal and external surfaces deviate slightly from the channel walls and its rear edges are points lying on the channel walls. If the transformation given by Eq. (9) is applied to this cowling shape, assuming that its inner and outer contours lie on different Riemann sheets in the physical plane with a branch point at $z=i$, the so-transformed contour will depart slightly from the ζ axis in the w plane. Calling $\epsilon\tilde{f}$ the departure from the ζ axis, the following problem for the real stream function ψ can be formulated:

$$\nabla^2\psi=0 \tag{9}$$

$$\left.\frac{\partial\psi}{\partial\zeta}\right|_{\zeta,\epsilon\tilde f}=-\epsilon\dot{\tilde f}\left.\frac{\partial\psi}{\partial\eta}\right|_{\zeta,\epsilon\tilde f} \tag{9a}$$

$$\psi\Big|_{\infty}\to-\frac{U_b}{\pi}\tan^{-1}\frac{\eta}{\zeta} \tag{9b}$$

Assuming an expansion of the form $\psi=\psi_0+\epsilon\psi_1$ and substituting in Eq. (9), ψ_0 results from the field of a source at the origin of intensity $2U_b$, namely the Borda mouthpiece solution,

$$\psi_0=-\frac{U_b}{\pi}\tan^{-1}\frac{\eta}{\zeta} \tag{10}$$

ψ_1 is determined from

$$\nabla^2\psi_1=0 \tag{11}$$

$$\left.\frac{\partial\psi_1}{\partial\zeta}\right|_{\zeta,0}=\frac{U_b}{\pi}\left(\frac{\dot{\tilde f}}{\zeta}-\frac{\tilde f}{\zeta^2}\right) \tag{11a}$$

$$\psi_1\,|_{\infty}=\text{const} \tag{11b}$$

The boundary conditions in Eq. (11) indicate that the perturbed solution will be given by the field induced by a continuous distribution of sources of the form

$$q(\zeta)=\epsilon\frac{2U_b}{\pi}\left(\frac{\dot{\tilde f}}{\zeta}-\frac{\tilde f}{\zeta^2}\right) \tag{12}$$

Then the perturbation potential is

$$\Delta\tilde{\phi}_b=\frac{1}{2\pi}\int_0^\infty q(\zeta)\ln(w-\zeta)\,d\zeta \tag{13}$$

The complex velocity in the physical plane is

$$V=-\frac{U_b}{w-1}-\epsilon U_b\frac{w}{w-1}\left[\frac{1}{\pi}\int_0^\infty\frac{\dot{\tilde f}(\zeta)}{\zeta(\zeta-w)}d\zeta-\int_0^\infty\frac{\tilde f(\zeta)}{(\zeta-1)^2(\zeta-w)}d\zeta\right]+\frac{d\phi_p}{dz} \tag{14}$$

Analyzing the real and imaginary parts of the transformation given by Eq. (7), it is found that, in order for the first integral in Eq. (18) to converge, ϵf has to vanish at least like $\exp(-\pi\bar{x})$ at infinity. This is not a restriction since $f=0$ beyond the exhaust plane. To verify the convergence of the second integral in Eq. (14), consider the expansion valid for $\bar{x}\to 0$, $\zeta\to 1$,

$$\epsilon f(\bar{x})\sim\gamma\bar{x} \tag{15}$$

Using the real part of the transformation, Eq. (15) can be rewritten as

$$\epsilon\tilde f\sim\frac{(1-\zeta)^2}{\pi\gamma}(\sqrt{1+\gamma^2}-1) \tag{16}$$

Hence, provided Eq. (16) is valid, the second integral in Eq. (14) converges.

The component ϕ_p of the outer potential flow is computed from the entrainment of the primary jet by simulating the entrainment effect with a sink distribution on the symmetry axis, with local intensity proportional to the rate of change of the

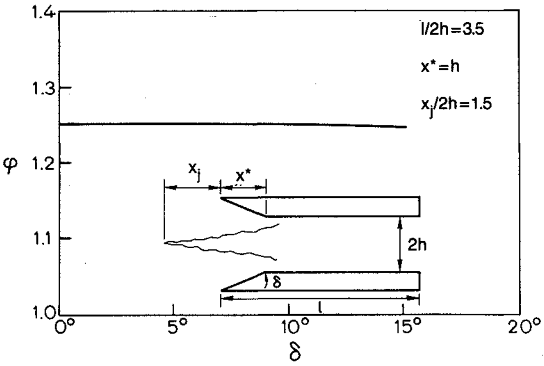

Fig. 4 Augmentor with wedge-shaped shroud.

mass flux involved in the excess velocity of the jet,

$$q_p = \lim_{y' \to \infty} \left[-2\frac{\partial}{\partial x}\int_0^{y'} u_1(x)e^{-\alpha(y^2/b^2)}\mathrm{d}y \right]$$

$$= -\sqrt{\frac{\pi}{\alpha}}\frac{\mathrm{d}}{\mathrm{d}x}(u_1 b) \tag{17}$$

Then

$$\phi_p = \frac{1}{2\pi^2}\int_{\zeta_j}^{\zeta_1} q_p(\zeta)\left[1+\frac{1}{\zeta}\right]\ell n(w-\zeta)\mathrm{d}\zeta \tag{18}$$

This equation can be solved approximately by discretizing q_p in segments of constant strength. The value of ζ_1 can be chosen close to the right end of region 1.

Viscous-Inviscid Matching

The matching process contains two loops, one that matches the exit pressure to atmospheric value and another that insures that the growth rate of the inner flow is compatible with the external field in region 1. The first is an outer loop which consists in finding the root of

$$p_e(m_j) - p_{\mathrm{atm}} = 0 \tag{19}$$

which is easily achieved with Newton's method.

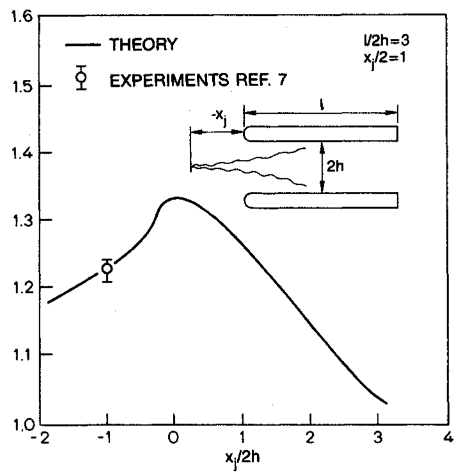

Fig. 5 Effect of primary nozzle position.

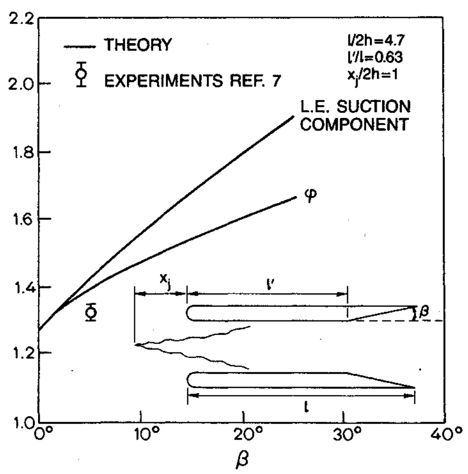

Fig. 6 Effect of diffuser angle.

The second, inner loop accomplishes the viscous-inviscid matching in region 1. This is done in a boundary-layer sense by setting the external limit of the viscous flow solution equal to the internal limit of the inviscid solution:

$$u_0(x) = V(\bar{x} - \bar{x}_j + i0) \tag{20}$$

The thrust produced by the pressure acting on the shroud is computed by applying the Blassius theorem to the Borda component of the external potential flow, performing the integration on a small, indented path around the leading edge of the basic straight channel, and then adding the pressure forces acting on the diffuser walls,

$$T = i\oint\left(\frac{\mathrm{d}\phi_b}{\mathrm{d}z}\right)^2 \mathrm{d}z + 2\int_\Omega p\mathrm{d}\Omega \tag{21}$$

where Ω is the vertical projection of the diffuser wall area. With the definition of thrust augmentation $\varphi = 1 + T/m_j$, it results in

$$\varphi = 1 + \frac{\rho U_b^2}{m_j} + \frac{2}{m_j}\int_\Omega p\mathrm{d}\Omega \tag{22}$$

Wedge-Shaped Shroud

A case where Eq. (14) can be evaluated analytically is given by the shroud shown in Fig. 4. In this case,

$$V = -\frac{U_b}{w-1} - \delta U_b \frac{w}{w-1}\left[\frac{1}{\pi w}\ell n\frac{\zeta^*(1-w)}{\zeta^*-w} - \bar{x}^*\left(\frac{\zeta}{(w-1)(\zeta^*-1)} + \frac{1}{(w-1)^2}\ell n\frac{\zeta^*-w}{w(\zeta^*-1)}\right) + \frac{1}{\pi}\int_{\zeta^*}^1 \frac{1-t+\ell n t}{(t-1)_2(t-w)}\mathrm{d}t\right] \tag{23}$$

This expression can be viewed as a first-order expansion of the inviscid field in powers of the wedge angle δ. Figure 4 shows the effect of wedge angle on augmentation. It is concluded that in a first-order analysis the particulars of the inlet shape are not important.

Straight-Walled Augmentor

The theory is applied to an augmentor with a shroud consisting of two thick flat plates as shown in Fig. 5 and the results are compared against the findings of Ref. 7. Although such augmentors have thick walls, the results of the previous

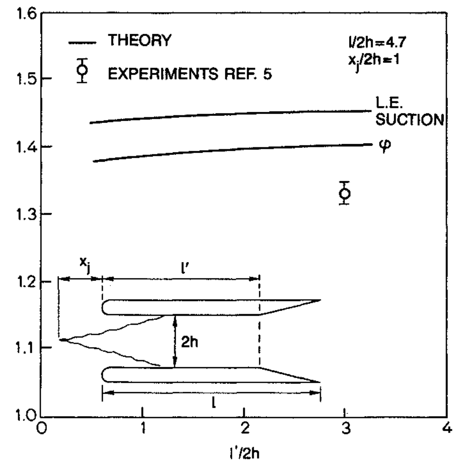

Fig. 7 Effect of diffuser length.

section suggest that the walls can be idealized as thin plates. This was done to obtain the results below.

Figure 5 shows the predicted thrust augmentation as a function of the primary nozzle position. It can be seen that the augmentation shows a maximum for a location of the primary nozzle near the inlet plane. Similar behavior has been observed experimentally.[1] Figure 6 shows the effect of the diffuser angle on augmentation. The leading-edge suction component of the augmentation is shown for illustration. For practical diffuser angles, the negative contribution of the diffuser pressure to the augmentation is less than 10%. The effect of keeping the diffuser area ratio constant and varying the position where the diffuser begins is demonstrated in Fig. 7. It can be seen that the length of the diffuser has very little influence on performance. This suggests that diffuser length could be chosen almost entirely on separation considerations, a conclusion supported by experiments.[1]

Conclusions

A methodology for the calculation of two-dimensional augmentor performance was developed, which, combining analytical and integral methods, allows for a fast and economical computation particularly suited for parametric studies. Because boundary layers are not taken into account, the calculations are limited to separation-free configurations. The most important limitation in the internal flow treatment is the modeling of the Reynold's stress. Although the eddy viscosity model used here appears satisfactory for global estimations, further improvement, particularly in the local quantities, should result from upgrading the stress model. Results were tested against one particular augmentor configuration studied experimentally at the Jet Propulsion Laboratories, with predicted performance within 10% of the measured values.

References

[1]Porter, J. L. and Squyers, R. A., "A Summary/Overview of Ejector Augmentor Theory and Performance," Vols. I and II, Vought Corp., ATC Rept. R-91100-9CR-47, 1981.

[2]Hickman, K. E., Hill, P. G., and Gilbert, G. B., "Analysis and Testing of High Entrainment Single-Nozzle Jet Pumps with Variable Area Mixing Tubes," NASA CR 2067, June 1972.

[3]Bevilaqua, P. M. and McCullough, J. K., "Entrainment Method for V/STOL Ejector Analysis," AIAA Paper 76-419, July 1976.

[4]Bevilaqua, P. M., "Lifting Surface Theory for Thrust Augmenting Ejectors," *AIAA Journal*, Vol. 16, May 1978, pp. 475-481.

[5]Bevilaqua, P. M. and DeJoode, A. D., "Viscid/Inviscid Interaction Analysis of Thrust Augmenting Ejectors," *Workshop on Thrust Augmenting Ejectors*, NASA CP 2093, Sept. 1979.

[6]Bevilaqua, P. M., Woan, C. J., and Shum, E. F., "Viscid/Inviscid Interaction Analysis of Ejector Wings," *Proceedings of the Ejector Workshop for Aerospace Applications*, AFWAL-TR-82-3059, Jan. 1982, pp. 868-877.

[7]Bernal, L. and Sarohia, V., "Entrainment and Mixing in Thrust Augmenting Ejectors," NASA CR 170027, Feb. 1982.

[8]Tavella, D. and Roberts, L., "Viscous-Inviscid Aerodynamic Analysis of Two-Dimensional Thrust Augmentors," NASA CR 177321, March 1984.